Sensing and actuating capabilities of a shape memory polymer composite integrated with hybrid filler

2010 Smart Mater. Struct. 19 065014

(http://iopscience.iop.org/0964-1726/19/6/065014)

Smart Mater. Struct. **19** (2010) 065014 (7pp) doi:10.1088/0964-1726/19/6/065014

Sensing and actuating capabilities of a shape memory polymer composite integrated with hybrid filler

Haibao Lu[1], Kai Yu[1], Yanju Liu[2] and Jinsong Leng[1,3]

[1] Centre for Composite Materials and Structures, Science Park of Harbin Institute of Technology (HIT), No. 2 YiKuang Street, PO Box 3011, Harbin 150080, People's Republic of China
[2] Department of Astronautical Science and Mechanics, Harbin Institute of Technology (HIT), No. 92 West Dazhi Street, PO Box 301, Harbin 150001, People's Republic of China

E-mail: lengjs@hit.edu.cn

Received 10 February 2010, in final form 11 April 2010
Published 4 May 2010
Online at stacks.iop.org/SMS/19/065014

Abstract

In this paper, hybrid fillers, including carbon black (CB) and chopped short carbon fibers (SCF), are integrated into a styrene-based shape memory polymer (SMP) with sensing and actuating capabilities. The hybrid filler is expected to transform insulating SMP into conducting. Static mechanical properties of the SMP composites containing various filler concentrations of hybrid filler reinforcement are studied first, and it is theoretically and experimentally confirmed that the mechanical properties are significantly improved by a factor of filler content of SCF. The excellent electrical properties of this novel type of SMP composite are determined by a four-point-probe method. As a consequence, the sensing properties of SMP composite filled with 5 wt% CB and 2 wt% SCF are characterized by functions of temperature and strain. These two experimental results both aid the use of SMP composites as sensors that respond to changes in temperature or mechanical loads. On the other hand, the actuating capability of SMP composites is also validated and demonstrated. The dynamic mechanical analysis result reveals that the output strength of SMP composites is improved with an increase in filler content of SCF. The actuating capability of SMP composites is subsequently demonstrated in a series of photographs.

(Some figures in this article are in colour only in the electronic version)

1. Introduction

Smart materials have attracted a great deal of interest in recent years. Their applications cover non-destructive evaluation [1], dynamics control and shape control [2], etc. Shape memory polymers (SMPs) are one candidate for actuation material in the field of shape control.

SMPs are the second important group of shape memory materials. Like SMAs, they have the capability of changing their shapes in response to an external stimulus. The most common ones are temperature or thermo-responsive SMPs, which typically consist of two polymer components and two phases: one with a higher melting temperature than the other. The glass transition temperature (T_g) is the reference point where the higher temperature component starts to melt. When heated above T_g, the SMPs are soft and rubbery, and easy to change shape. When subsequently cooled below T_g, they will retain the given shape (shape fixing characteristic). When heated again above T_g, the materials autonomously return to the original 'parent' shape [3, 4].

SMPs have gained substantial interest in the community of deployable space structures, owing to their superior structural versatility, lower manufacturing cost, easier pretreatment procedure, larger recoverable deformation and lower recovery temperature [5–9]. However, these materials in unreinforced form are unsuitable for the proposed applications, which require high stiffness and recovery force [10]. Also, the need

[3] Author to whom any correspondence should be addressed.

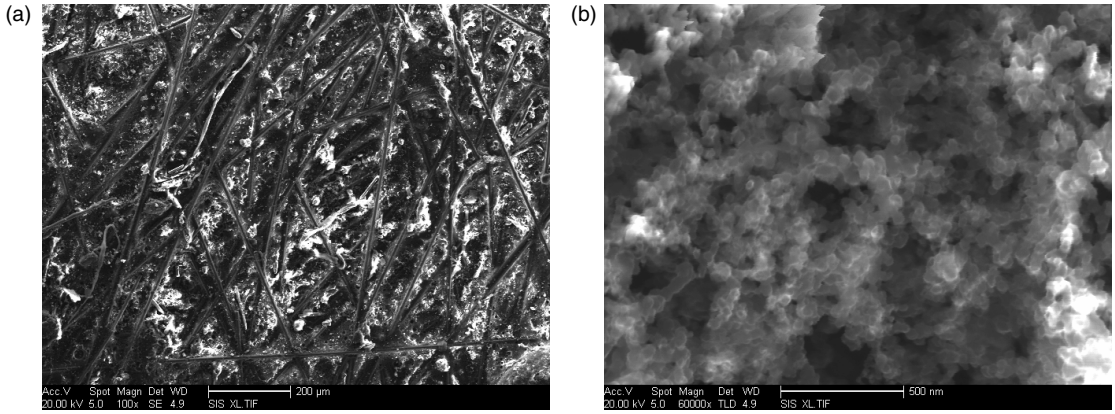

Figure 1. The morphologies of a SCF–SMP composite specimen observed by SEM (SMP with 2 wt% SCF and 5 wt% CB particles). (a) Morphologies of SCF fillers and (b) morphologies of CB particles.

to induce SMPs by non-thermal stimuli has led to increased usage of conductive fillers, such as conductive particles, carbon particles and conductive fibers [11]. In comparison to micro-sized reinforcements, nanoreinforcements dispersed into SMPs hold great promise as materials that provide nonlinear improvements in their thermo-mechanical and dynamic mechanical properties [12–15].

The short-carbon-fiber-reinforced SMP composite (SCF–SMP) consists of short fibers dispersed into an SMP matrix. Compared with SMP composites reinforced by conductive particles or long conductive fibers, SCF–SMP has many unique advantages, such as low cost, easy of fabricating complex parts and isotropic nature, and hence it is an ideal choice for large-scale production. Consequently, it is also suitable for lightly loaded component manufacturing. Aligned SFC–SMPs can be produced by injection molding and extrusion processes which have excellent in-plane mechanical properties, whereas a randomly oriented SCF–SMP composite shows a quasi-isotropic nature in macroscopic scale. The most widely used composite material should be the randomly oriented SCF–SMP composite due to its comparatively easy production process.

The randomly oriented SCF–SMP composite can be regarded as a conductive polymer which has found extensive potential applications in the fields of microsensors and micro-actuators, providing cheaper, accurate and faster alternatives to devices already on the market. Based on these, various chemical sensors and biosensors with remarkable specifications will be developed and applied in medicine for fast bio-diagnostic systems. Conductive polymer-based actuators also seem to hold great promise for future applications, due to their high strength and low energy consumption [9, 16].

In the following sections, specimens with different chopped fiber weight fractions are prepared first and their morphologies are observed by scanning electron microscope (SEM). Then, their mechanical properties are studied both theoretically and experimentally, and their electrical properties are also investigated by related experiments. The results will provide meaningful guidance for further design and performance evaluation of SCF–SMP composites.

2. Investigated materials and fillers

The SMP (Veriflex®S VF 62, supplied from Cornerstone Research Group, Inc., Dayton, OH, USA) is a styrene-based resin, with a density of 0.92 g cm^{-3}. Veriflex VF 62 is a two-part, fully formable thermosetting SMP resin system. The resin is engineered with a glass transition temperature (T_g) of 62 °C. The cured Veriflex VF 62 resin has unique 'shape memory' properties. When heated above the glass transition temperature (T_g), it changes from a rigid plastic to an elastic rubber. Carbon black (CB) (AX-010) particles are purchased from GuangZhou Sunny Plaza Trading Co., Ltd, with a density of 1.80 g cm^{-3}. The CB has a mean aggregate size of 4 μm, mean domain size (x-ray diffraction) of 18–20 nm and a domain content of 65 wt%. The particles have an electrical volume resistivity of 5×10^{-2} Ω m at 20 °C. The short carbon fibers (SCF) are cut from a continuous carbon fiber (T700), with lengths ranging from 0.5 to 3 mm, a diameter of 7 μm, stress strength of 4900 MPa and volume resistivity of 1.5×10^{-4} Ω m at room temperature.

The material preparation follows four steps: (1) shape memory resin is mixed with a crosslinking agent at a fixed proportion of 24:1 in weight. (2) CB and SCF were added to the resin mixture in the necessary proportions, followed by adding acetic acid ester to aid the viscosity of the mixture, due to the viscosity problem always making the mixture too thick to release air bubbles, followed by a high shear mixing and a high energy sonication (VCX750, Sonics&Materials, Inc.). (3) The mixture was treated with a vacuum pump to completely remove air bubbles. (4) The resin mixture is transferred into a closed mold. The resin mixture was cured at a ramp of approximately 1 °C min^{-1} from room temperature to 75 °C. The sample was then held at 75 °C for 3 h before being ramped to 90 °C at 15 °C/180 min. Finally, it was ramped to 110 °C at 20 °C/120 min.

3. Results and discussion

3.1. Morphology observation by scanning electron microscope

Figure 1 shows the morphologies of the developed SCF–SMP composite specimen with an SCF content of 2 wt% and CB

particle content of 5 wt%. Scanning electron microscopy (SEM) observations showed that the SCF fillers distribute randomly and separately from each other in the thermoset styrene-based SMP matrix. SCFs may be considered to provide conductive pathways and promote relatively long distance charge transfer, leading to the easy formation of continuous conductive networks, resulting in a significant drop in electrical resistance. These SCFs are expected to play a prominent role in enhancing the electrical properties of SMP composites in comparison with the particle aggregates. The numerous interconnections between the SCF fibers form conductive networks in the composite and can be used to explain the excellent electrical conductivity of the composites filled with SCF. Meanwhile, figure 1(b) shows the morphology of CB particles in the specimen. Clearly, the particle fillers distribute uniformly in the SMP matrix, aggregating as clusters instead of absolutely separating from each other. In this way, the CB particles will act as nodes among the fibers, and local conductive pathways will also be formed in the composite, which will improve the orientation of the short fibers. Because of the large amount of conductive channels formed in the composite, the resistivity may be relatively low and stable.

3.2. Mechanical properties' measurement

Unlike continuous fiber SMP composites, the external loads are not directly applied to the fibers in SCF–SMP composites. The load applied to the matrix material is transferred to the fibers via fiber ends and the surfaces of fibers. As a consequence, the mechanical properties of SCF–SMP composites greatly depend on the fiber length and diameter (i.e. fiber aspect ratio = length/diameter of fiber) of the fibers. Further, several factors such as fiber orientation, weight fraction, fiber spacing, fiber packing arrangement and curing parameters also significantly influence the properties of the SCF–SMP composites [17, 18]. During the past few decades, there has been a significant development in property prediction models of short-fiber-reinforced composites based on micro- and macro-mechanics. Some empirical relationships are also available to be used in the determination of the approximate properties of random short-fiber composites [19].

Typically, the modified Halpin–Tsai equation [20] can be expressed as follows:

$$E_c = \tfrac{3}{8}E_1 + \tfrac{5}{8}E_2 \tag{1}$$

where

$$E_1 = E_m\left(\frac{1+\xi\eta_1 v_f}{1-\eta_1 v_f}\right), \qquad E_2 = E_m\left(\frac{1+\xi\eta_2 v_f}{1-\eta_2 v_f}\right),$$

$$\eta_1 = \frac{\left(\frac{E_f}{E_m}\right)-1}{\left(\frac{E_f}{E_m}\right)+2(l/d)} \quad \text{and} \quad \eta_2 = \frac{\left(\frac{E_f}{E_m}\right)-1}{\left(\frac{E_f}{E_m}\right)+2}.$$

In this relationship, the E_c, E_m and E_f are the Young's modulus of composite, matrix and reinforcement fiber, respectively. l is average fiber length and d is the diameter of the fiber. Halpin suggested that $\xi = 2(l/d)$ gives good predictions from the proposed relationship.

However, the Young's modulus in the former empirical relationship is based on one-component materials, which can be regarded as a basic material constant. However, in our study, the CB particles are doped into the SMP resin before it is used as the composite matrix. The mole number per unit of the material will be subsequently changed. Because of the large influence of CB particles on the material properties of the SMP, especially the tensile strength and elastic modulus, the Young's modulus of the SMP doped with CB particles will be recalculated in the following study.

If the CB particles are treated as molecules in a solvent, a swelling effect will be generated in the mixed solution after the particle fillers are doped into the SMP. Based on rubber elasticity theory, the force per unit area can be expressed as follows:

$$\sigma = nRT\frac{\overline{r_i^2}}{\overline{r_0^2}}\left(\alpha - \frac{1}{\alpha^2}\right). \tag{2}$$

In this equation, L_0 is increased to L, $\alpha = L/L_0$ is the elongation ratio and RT is the gas constant times absolute temperature. The two quantities $\overline{r_0^2}$ and $\overline{r_i^2}$ represent the same chain in the network and uncross-linked states, respectively. Generally, the quantity $\overline{r_i^2}/\overline{r_0^2}$ approximately equals unity. The quantity n represents a network made up of n chains per unit volume.

Several other relationships may be derived immediately, since Young's modulus is the function of state:

$$E = L\left(\frac{\partial\sigma}{\partial L}\right)_{T,V} \cong 3n\frac{\overline{r_i^2}}{\overline{r_0^2}}RT. \tag{3}$$

Therefore

$$E = nRT\frac{\overline{r_i^2}}{\overline{r_0^2}}\left(\alpha + \frac{2}{\alpha^2}\right) \cong 3n\frac{\overline{r_i^2}}{\overline{r_0^2}}RT. \tag{4}$$

If a polymer network is swollen with a 'solvent' (it does not dissolve), the detailed effect has two parts.

(1) The effect on $\overline{r_i^2}/\overline{r_0^2}$. The quantity $\overline{r_i^2}$ increases with the volume V to the two-thirds power, while $\overline{r_0^2}$ remains constant. The work done on the polymer network is

$$\left(\frac{\overline{r_i^2}}{\overline{r_0^2}}\right) = \left(\frac{V}{V_0}\right)^{2/3}\left(\frac{\overline{r_i^2}}{\overline{r_0^2}}\right)^{*} = \frac{1}{v_2^{2/3}}\left(\frac{\overline{r_i^2}}{\overline{r_0^2}}\right)^{*} \tag{5}$$

where '*' represents the swollen state and v_2 is the volume ratio of the polymer in the not-swollen and swollen stages. Of course, v_2 is less than unity, as is commonly experienced.

(2) The effect on the number of network chain segment concentration, n. The quantity n gives the expression:

$$\left(\frac{V}{V_0}\right)n = v_2 n = n_s \tag{6}$$

where n_s is the chain segment concentration in the swollen stage. By substituting equations (5) and (6) into (4) we obtain empirical relationships of

$$E = 3nv_2^{1/3}\frac{\overline{r_i^2}}{\overline{r_0^2}}RT. \tag{7}$$

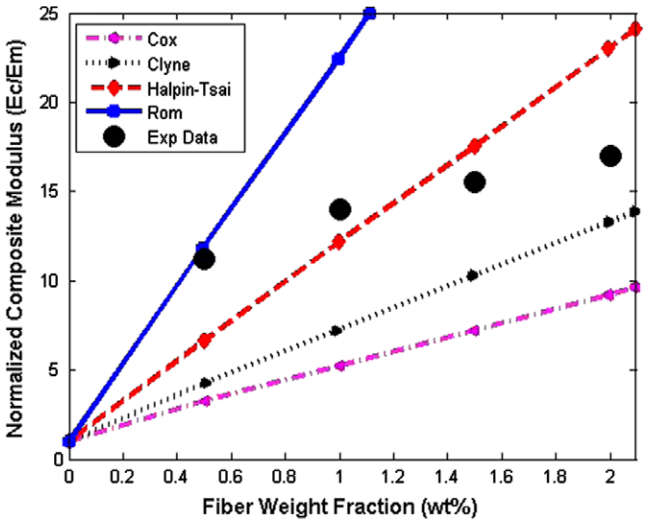

Figure 2. Curves of normalized composite modulus versus fiber weight fraction of short carbon fibers.

Until now, the equivalent modulus of the SMP material doped with CB particles is worked out. By submitting it into the existing property prediction theories of short-fiber-reinforced composites, the elastic modulus of the SCF–SMP composite can be calculated.

Isothermal static stress–strain tests are conducted to test the mechanical properties of the conducting composite. Tensile tests are performed by using a Zwick/Roell servo-mechanical test frame with a series digital controller. An Instron clip-on extensometer is used for strain measurement in tensile tests, while the test frame's extension sensor is used for the shear tests. In calculation of the experimental data, the engineering stress and strain are used. The strain is calculated by the ratio of the elongation obtained by the crosshead displacement to the gauge length (50 mm).

Figure 2 shows a comparison between the experimental results and theoretical predictions in the mechanical analysis of the SCF–SMP composite. In this image, the normalized composite modulus consist of the composite modulus divided by the modulus of pure SMP material doped with CB particles. Each value in the theoretical model is calculated by the former developed analysis method. Meanwhile, the four experimental data correspond to the maximum strain in the isothermal static stress–strain tests of each specimen. It is clearly seen that the composite modulus is greatly enhanced by adding short carbon fibers, and it increases significantly with increasing relative short-carbon-fiber weight fraction. Meanwhile, the calculation results in the Rom, Cox and Clyne models are relatively different from the experimental values. These deviations get more obvious with the increase in fiber weight fraction. However, predictions in the Halpin–Tsai model show a closer fit with the experimental results, and a similar slope of the experimental data and the Halpin–Tsai model can also be observed, indicating that, with an increase in fiber weight fraction, the Halpin–Tsai model can provide a more precise prediction than the other models during the mechanical analysis of the SCF–SMP composite.

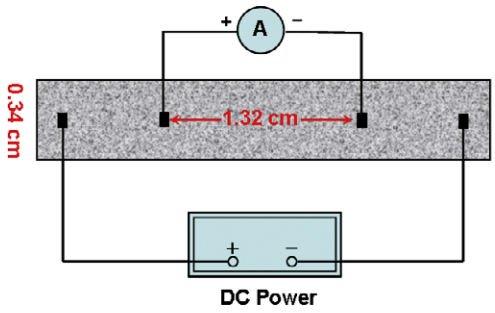

Figure 3. Schematic illustration of the measurement for a rectangular specimen.

3.3. Sensing capabilities of SMP composite with hybrid filler

Through our previous research work, it is found that testing results of the electrical properties for SCF–SMP composites are different with varying contact positions between the electrodes and the specimen. To avoid incidental error, the Van De Pawn four-point-probe method is used in this study. A Keithley 2400 resistivity tester and Keithley 2000 picoammeter/voltage source are used to measure the volume resistivity of a rectangular sheet (1.32 cm × 0.34 cm × 0.16 cm). The experimental set-up is shown in figure 3. The volume resistance is 56.0 Ω at a temperature of 28.8 °C, and the volume resistivity 2.32 Ω cm is obtained.

One of the thermo-sensitive effects in conducting polymer composites is the resistance changing with increasing temperature within a certain temperature range, which is known as the positive temperature coefficient (PTC) effect. The PTC effect for conducting polymer composites depends remarkably on the properties of polymer matrices and conducting fillers. In this work, the dependence of the resistance on temperature in the range from 30 to 100 °C is investigated with a constant heating rate of 1.0 °C min^{-1}. Meanwhile, four specimens with different SCF weight fractions (0.5, 1, 1.5 and 2 wt%) are tested simultaneously for comparison.

In the process of temperature-dependent resistance tests, with the temperature varying, the main factors determining the resistance of the SCF–SMP composite are electron movement, molecular vibration and expandability. These three factors increased with increasing temperature. While the electron movement can reduce the resistance of the composite materials, expandability will increase the distance between conductive particles and the molecular vibration will block the electron movement, which will both increase the resistance of the composite.

As is shown in figure 4, at the same temperature, the resistance of the specimen decreases remarkably with the increase in fiber weight fraction. This is because the greater the weight fraction of the short fibers, the more continuous conductive pathways will be generated in the specimen. All the specimens have a similar resistance trend. From 35 to about 70 °C, the resistance of each specified specimen increases slowly with increasing temperature. Then, after 70 °C, its resistance increases abruptly with increasing temperature. It shows a classical positive temperature coefficient (PTC) effect.

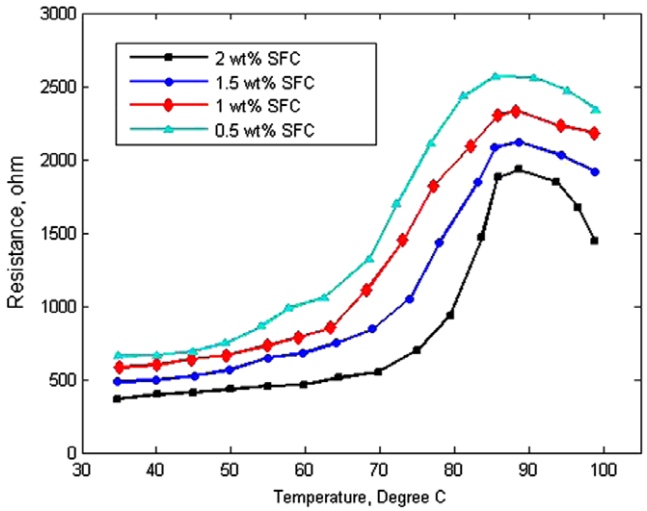

Figure 4. Values of resistance versus temperature for the SCF–SMP composite.

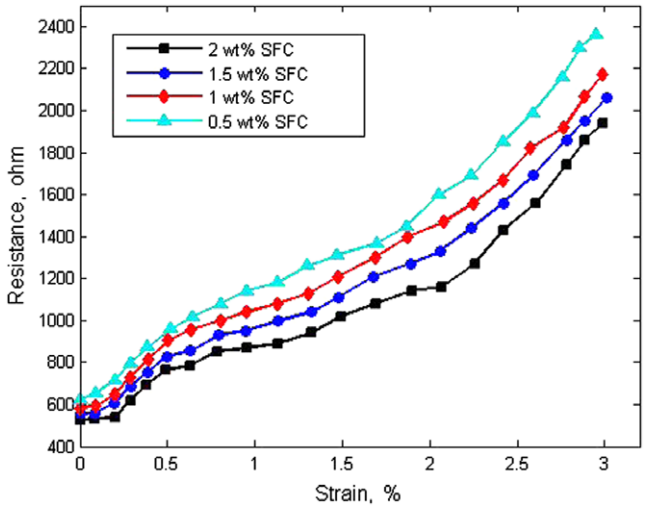

Figure 5. Values of resistance versus strain for SCF–SMP composite.

But with temperature increasing above 70 °C, the volume resistance decreased obviously. It showed a classical negative temperature coefficient (NTC) effect.

In the following test, the resistance of the conducing polymer composite changes with altering strain. The dependence of the resistance on the strain in the range from 0% to 3% was investigated at a constant rate. Similar to the former study, all four specimens with different SCF weight fractions are also tested for comparison.

Figure 5 shows curves of resistance values versus strain for the SCF–SMP composite. Accompanied by outer loading or shape changing, the phenomenon of strain-dependent resistance for conducting SCF–SMP composites will occur, and hence the resistance changing directly or indirectly will reveal the outer factors' focus on them. At the same strain rate, the specimen with a higher fiber weight content has a lower resistance due to the increased continuous conductive pathways. The detailed resistance variation process for each specimen can be expressed as follows: at the beginning, with increasing strain, the distance of CB particles and SCF fillers are increased gradually, so the charge transport over a small distance is destroyed. Because the outer force drives the CB particles and their aggregates to break away from the SCF fillers, the contact situation between CB and SCF is influenced and the electron transport distance is also changed. Consequently, new conductive paths are constructed, which can somewhat compensate for conductivity losses resulting from increased distances between conductive fillers. With a further increase in the strain, the change transport over large distances is destroyed. In this case, resistance increases drastically.

3.4. Actuating capability of SMP composite with hybrid filler

In the following section, the actuating properties of the conducting SCF–SMP composite are studied by introducing a parameter called recovery strength, which shows the stress generated per unit of strain. In the previous research work [10], DMA tests were conducted to test the storage and loss modulus of the pure and SCF-reinforced SMP materials at different temperatures. The experiments were performed using an NETZSCH DMA 242C to determine the dynamic mechanical properties of the SMP composites. All experiments were conducted at a constant heating rate of 5.0 K min^{-1}. The oscillation frequencies were 1.0 Hz. The sample was investigated from −50 to 120 °C. The dimensions are 75.0 mm × 4.73 mm × 1.10 mm. The proposed recovery strength of the SCF–SMP composite or pure SMP can be expressed as follows:

$$E_{\mathrm{R}} = \sqrt{E_{\mathrm{S}}^2 + E_{\mathrm{L}}^2} \tag{8}$$

where E_{R} represents the shape recovery strength, E_{S} is the storage modulus and E_{L} is the loss modulus.

After calculation, curves of recovery strength versus different experimental temperatures are obtained. Three specimens, pure SMP, SMP with 5 wt% CB particles and 1 wt% SCF fillers, and SMP with 5 wt% CB particles and 2 wt% SCF fillers are adopted for comparison. It is presumed that the three specimens show the shape recovery performance within the temperature range of 30–70 °C.

As is shown in figure 6, for each specimen, the recovery strength decreases slowly at the beginning, and then a sharp decrease is observed around 50 °C. This is because the molecular chains are frozen in the materials when the temperature is relatively low, and the shape recovery effect cannot be fully expressed at this stage. Therefore, the elastic modulus of the materials is relatively high and more stress will be generated per unit of strain. In other words, if the material is fixed and exposed to external forces, more resistance stress will be generated inside the material. With a temperature increase, the molecular chains in the materials begin to separate and the locomotory units start to move, resulting in the decreasing elastic modulus. Even though the shape memory materials start to show their shape memory effect, the recovery strength decreases drastically since the materials begin to show viscoelasticity.

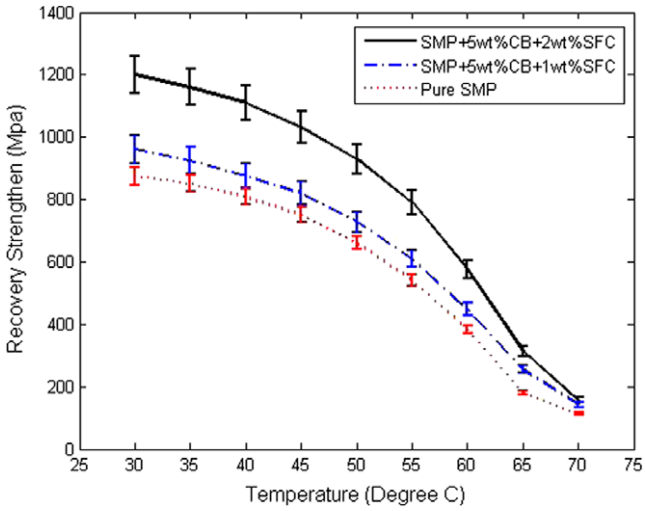

Figure 6. Curves of recovery strength versus experimental temperature.

Moreover, under the same temperature, the recovery strength increases considerably with increasing SCF weight fraction, indicating that the SCF filler can reinforce the SMP material in a positive way, not only for its mechanical properties, but also its actuating capability. The proposed conducting SCF–SMP composites show more potential and suitability for the design and manufacture of smart actuators.

The shape recovery behavior of SCF–SMP composite materials being driven by electrical current has also been carried out. It is found that the chopped carbon fibers significantly reduce the electrical resistivity, and then the particulate filler inhomogeneously improves the electrical properties and thermal conductivity. This synergetic effect has been shown to drive the shape recovery of SCF–SMP composites and actuate the motion of a table tennis ball being recorded simultaneously by a video camera, which is shown in figure 7. The specimen used, which contained 5 wt% CB and 2 wt% SCF (the length of chopped carbon fibers is 3 mm), is about 112 mm × 23.2 mm × 4 mm. The electrical conductivity 2.32 S cm of the composite which can be considered as a conductor is calculated by the Van De Pawn method. The shape transition in a DC field of 30 V is documented with a digital camera. In 70 s, the starting conversion of the flexural shape is observed to be completed. The final shape is close to the original plane shape with some remaining flexion due to the self-gravity of the material and the friction between the soft polymer and the glass plate. The rate of shape recovery is strongly dependent on the magnitude of the applied voltage and the electrical resistivity of the composite. Three other effects also play a role: (1) with the increase in fiber weight fraction, there is less shape memory material to recover, and the rate of recovery will decrease; (2) the disturbance of the shape memory material by the dispersed phase results in a decreasing rate of recovery and (3) the storage of elastic deformation energy in the SCF will increase the rate of recovery. Furthermore, all the composites filled with chopped carbon fibers (content of 0.5–2 wt%) behave like conductors in this study, and the shape recovery of which with dimensions of 112 mm × 23.2 mm × 4 mm can be driven by a low voltage from 20 to 100 V.

4. Conclusions

This paper presents a systematic study of the mechanical and electrical properties of SCF–SMP composites. These basic investigations integrate this novel SMP composite with its sensing and actuating capabilities. There are three conclusions to be drawn as follows.

(1) The conductive network is virtually formed resulting in a sharp transition from insulating to electrically conductive, while the inherent fibrillar form of the SCF fillers has a higher tendency to form a three-dimensional network in the conductive composites and promote relatively long distance charge transfers.

(2) The mechanical properties of the SCF–SMP composite have a determinable relationship with the conductive fillers. The fibrous fillers enhance the mechanical properties of the SCF–SMP composites more significantly than the particulate fillers. Furthermore, the rubber elastic theory is employed to characterize the effect of hybrid fillers on the elastic modulus of the SMP composite. This numerical result has been demonstrated to be in good agreement with static mechanical results.

(3) Due to the synergetic effect of the electrically conductive hybrid and the shape memory effect of the SMP composite, the developed SMP composites are integrated

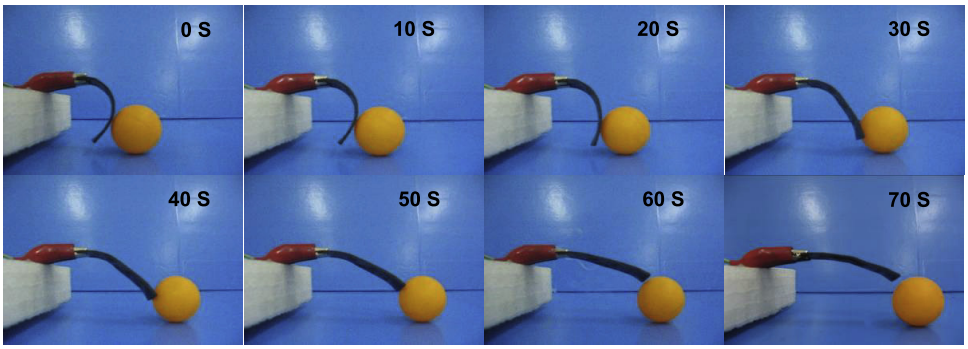

Figure 7. Series of photographs showing the macroscopic shape memory effect of SMP/5CB/2SCF composite and actuating the motion of a table tennis ball. The permanent shape is a plane stripe of composite material and the temporary shape is deformed as a right-angle shape.

with sensing and actuating capabilities. Many potential applications of this novel SMP composite have been explored, especially in multifunctional SMP composite with sensing and actuating capabilities.

References

[1] Lendlein A, Jiang H, Jünger O and Langer R 2005 Light-induced shape-memory polymers *Nature* **434** 879–82

[2] Leng J S and Asundi A 1999 Active vibration control system of smart structures based on FOS and ER actuator *Smart Mater. Struct.* **8** 252–6

[3] Koerner H, Price G, Pearce N A, Alexander M and Vaia R A 2004 Remotely actuated polymer nanocomposites—stress-recovery of carbon-nanotube-filled thermoplastic elastomers *Nat. Mater.* **3** 115–20

[4] Liu Y J, Lv H B, Lan X, Leng J S and Du S Y 2009 Review of electro-activate shape-memory polymer composite *Comput. Sci. Technol.* **69** 2064–8

[5] Lv H B, Leng J S, Liu Y J and Du S Y 2008 Shape-memory polymer in response to solution *Adv. Eng. Mater.* **10** 592–5

[6] Leng J S, Lv H B, Liu Y J and Du S Y 2008 Comment on 'Water-driven programmable polyurethane shape memory polymer: demonstration and mechanism' *Appl. Phys. Lett.* **92** 206105

[7] Lu H B, Liu Y J, Leng J S and Du S Y 2009 Qualitative separation of the effect of solubility parameter on the recovery behavior of shape-memory polymer *Smart Mater. Struct.* **18** 085003

[8] Leng J S, Lu H B, Liu Y J, Huang W M and Du S Y 2009 Shape-memory polymer—a novel class of smart material *MRS Bull.* **34** 848–55

[9] Zhou B and Leng J S 2009 A glass transition model for shape memory polymer and its composite *Int. J. Mod. Phys.* B **23** 1248–53

[10] Leng J S, Lv H B, Liu Y J and Du S Y 2007 Electro-activate shape memory polymer filled with nanocarbon particles and short carbon fibers *Appl. Phys. Lett.* **91** 144105

[11] Lan X, Liu Y J, Lv H B, Leng J S and Du S Y 2009 Fiber reinforced shape-memory polymer composite and its application in a deployable hinge *Smart Mater. Struct.* **18** 024002

[12] Leng J S, Lv H B, Liu Y J and Du S Y 2008 Synergic effect of carbon black and short carbon fiber on shape memory polymer actuation by electricity *J. Appl. Phys.* **104** 104917

[13] Leng J S, Huang W M, Lan X, Liu Y J and Du S Y 2008 Significantly reducing electrical resistivity by forming conductive Ni chains in a polyurethane shape-memory polymer/carbon black composite *Appl. Phys. Lett.* **92** 204101

[14] Weigel T, Mohr R and Lendlein A 2009 Investigation of parameters to achieve temperatures required to initiate the shape-memory effect of magnetic nanocomposites by inductive heating *Smart Mater. Struct.* **18** 025011

[15] Pan G H, Huang W M, Ng Z C, Liu N and Phee S J 2008 The glass transition temperature of polyurethane shape memory polymer reinforced with treated/non-treated attapulgite (playgorskite) clay in dry and wet conditions *Smart Mater. Struct.* **17** 045007

[16] Leng J S, Lan X, Liu Y J, Du S Y, Huang W M, Liu N and Phee S J 2008 Electrical conductivity of shape memory polymer embedded with micro Ni chains *Appl. Phys. Lett.* **92** 014104

[17] Lu H B, Liu Y J, Gou J, Leng J S and Du S Y 2010 Synergistic effect of carbon nanofiber and carbon nanopaper on shape memory polymer composite *Appl. Phys. Lett.* **96** 084102

[18] Lu H B, Yu K, Liu Y J and Leng J S 2010 Mechanical and shape-memory behavior of shape-memory polymer composites with hybrid fillers *Polym. Int.* doi:10.1002/pi.2785

[19] Latifa S and Chakraborty S 2004 Effective moduli of random short fiber composite: a probabilistic study *J. Reinf. Plast. Compos.* **23** 751

[20] Epaarachchi J, Ku H and Gohel K 2009 A simplified empirical model for prediction of mechanical properties of random short fiber/vinylester composites *J. Compos. Mater.* **44** 779–88